Structural Engineering and Mechanics, *Vol. 55, No. 1 (2015) 111-135*
DOI: http://dx.doi.org/10.12989/sem.2015.55.1.111

Congestion effect on maximum dynamic stresses of bridges

Kianoosh Samanipour* and Hassan Vafai[a]

Department of Civil Engineering, Sharif University of Technology, Tehran, Iran

(Received May 1, 2014, Revised May 9, 2015, Accepted May 28, 2015)

Abstract. Bridge behavior under passing traffic loads has been studied for the past 50 years. This paper presents how to model congestion on bridges and how the maximum dynamic stress of bridges change during the passing of moving vehicles. Most current research is based on mid-span dynamic effects due to traffic load and most bridge codes define a factor called the dynamic load allowance (DLA), which is applied to the maximum static moment under static loading. This paper presents an algorithm to solve the governing equation of the bridge as well as the equations of motions of two real European trucks with different speeds, simultaneously. It will be shown, considering congestion in eight case studies, the maximum dynamic stress and how far from the mid-span it occurs during the passing of one or two trucks with different speeds. The congestion effect on the maximum dynamic stress of bridges can make a significant difference in the magnitude. By finite difference method, it will be shown that where vehicle speeds are considerably higher, for example in the case of railway bridges which have more than one railway line or in the case of multiple lane highway bridges where congestion is probable, current designing codes may predict dynamic stresses lower than actual stresses; therefore, the consequences of a full length analysis must be used to design safe bridges.

Keywords: bridge; dynamics; congestion; maximum dynamic stress; stress analysis; finite difference method; DLA (dynamic load allowance)

1. Introduction

One of the most important problems facing design and structural engineers is the cognition and analysis of dynamic behavior of bridges subjected to moving forces (moving loads, moving masses and moving vehicles). In general mechanics parlance the loads that vary in both time and space are called moving loads. For instance, transport engineering structures are subjected to such loads. In recent years increasingly higher speeds and weight of vehicles have had a great influence in all branches of transport. As a result, vibrations and dynamic stresses far larger than ever before occur in structures and media over or in which the vehicles move.

Jeffcott in 1929, Steuding in 1943 and Odman in 1951 studied first the influence of a moving mass on the dynamic response of a structure (Akin and Mofid 1989). Many approximations were involved in their solution which made it impractical. Fryba (1972) wrote a helpful book containing almost all of the previous work in the field of vibration of solids and structure under moving loads.

*Corresponding author, Ph.D. Candidate, E-mail: Kianoosh_samanipour@yahoo.com
[a]Professor, E-mail: vafai@sharif.edu

http://www.techno-press.org/?journal=sem&subpage=8 ISSN: 1225-4568 (Print), 1598-6217 (Online)

Zheng and Cheung (2000) studied the vibration of vehicles on compressed rails on a viscoelastic foundation. They utilized a theoretical and analytical approach to solve the problem considering resonance parameters as well. Other papers have been written considering acceleration of moving mass, friction between moving mass and bridge (Wang 1998), cantilever beams (Siddiqui *et al*. 1998), large free vibrations (Siddiqui *et al*. 2003), and curved beams (Wang 2005).

Dehestani *et al*. (2009) investigated critical influential speed for moving mass problems on the beams with different end conditions. In other research, Mofid *et al*. (2010), presented two methods to determine the dynamic behavior of viscoelastic beams subjected to moving mass. Cantero *et al*. (2009) calculated the maximum dynamic stress on simply supported bridges traversed by moving vehicles.

Bridge codes have different approaches in considering dynamic effects due to moving traffic. For example, the American Association of State Highway and Transportation Officials (AASHTO) (2012), defines a factor called DLA (Dynamic Load Allowance), which considers the dynamic effects of moving vehicles and applies them to the maximum static stresses. For fatigue and fracture the AASHTO proposes the DLA to be 1.15 and 1.33 for all other limits states for all spans (O'Connor and Shaw 2000). In the Eurocode EN 1991-2 (2003) different load models based on experimental results from a number of countries, are defined. For each load model, different dynamic factors obtained from numerical simulations are used. Dynamic effects are combined with static results to obtain characteristic values by using these dynamic factors.

During 2011 to 2014, many studies, particularly considering the moving oscillator effects on the bridge behavior, have been done in different universities and research institutions (Gasic *et al*. 2011), (Zhang *et al*. 2013), (Chang *et al*. 2014).

In summary, because of the importance of bridges safety, many researches and simulations are being carried out to predict the dynamic amplification factors by different universities and institutions all over the world. But congestion is not investigated well in previous studies and usually the researchers assume that the congestion is neglected. Furthermore, analyzing the influence of congestion with respect to variation of truck speeds, bridge spans and road profiles and its effect on variation of the dynamic amplification factors has many significances as well. In this paper, the problem definition is supplied and afterwards an algorithm to solve the governing equation of actual European trucks moving on different bridges considering congestion, is presented. The present work extends the scope of previous studies by considering actual truck moving instead of moving mass problem (Dehestani *et al*. 2009, Mofid *et al*. 2010) and by considering congestion for the beam loading (Cantero *et al*. 2009). The critical velocities for congestion of two trucks to get maximum beam dynamic stresses are numerically calculated.

In this paper, the following assumptions are made. First, the beam dynamic characteristics are described by Euler-Bernoulli beam equation. Furthermore, the beam is assumed to be of constant cross-section with uniform mass distribution and is hinged at both ends. Second, the effects of inertia for both the beam and the moving truck are taken into account with the gravitational effect of load. Third, the trucks move with two different but constant speeds and are guided in such a way that the probable uplifts of tires are considered in the analyses. The objectives of this investigation are: (1) to formulate the solution of the problem in the general form, (2) to present a practical and precise technique for determining the dynamic response of a Euler-Bernoulli beam, considering congestion, (3) to verifying the model with previous studies, and (4) to study the important factors such as moving truck velocity, congestion and beam length in the dynamic amplification factors which cause more dynamic stresses in bridges.

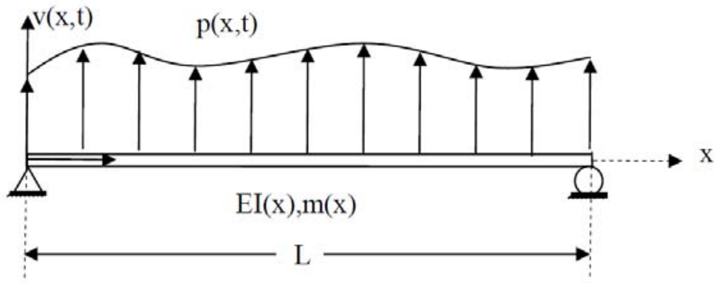

Fig. 1 Beam general model

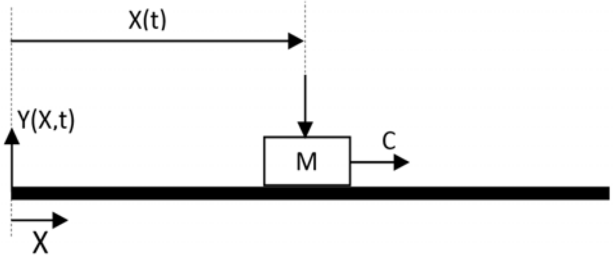

Fig. 2 Beam carrying moving load

2. Problem definition

For an Euler-Bernoulli beam under static load case, the governing equation is

$$EI\frac{\partial^4 y}{\partial x^4} = P(x) \tag{1}$$

Fig. 1 shows an Euler-Bernoulli beam carrying an oscillating load *P(x,t)* which can vary with time and location.

The equation of motion of the Euler-Bernoulli beam can be expressed in the form (Fryba 1972)

$$EI\frac{\partial^4 y}{\partial x^4} + 2\mu\omega_b\frac{\partial y}{\partial t} + \mu\frac{\partial^2 y}{\partial t^2} = P(x,t) \tag{2}$$

Where $y(x,t)$ is the vertical deflection of the beam at location x and instant t, I is the second moment of the area, E is the modulus of elasticity, ω_b is the damped circular frequency and μ is the constant mass per unit length of the beam.

Fig. 2 shows a moving object which is travelling at a constant horizontal velocity C along the beam.

The equation of motion of the Euler-Bernoulli beam for moving load case can be expressed in the form (Fryba 1972)

$$EI\frac{\partial^4 y}{\partial x^4} + 2\mu\mu_b\frac{\partial y}{\partial t} + \mu\frac{\partial^2 y}{\partial t^2} = -Mg \times \delta(x - X) \tag{3}$$

Where δ is the Dirac function.

If the mass of the moving object has been taken into account in writing the dynamic governing equation, the problem is in the form (Fryba 1972)

$$EI\frac{\partial^4 y}{\partial x^4}+2\mu\omega_b\frac{\partial y}{\partial t}+\mu\frac{\partial^2 y}{\partial t^2}=-M\left[\frac{\partial^2 y}{\partial t^2}+g\right]\delta(x-X) \tag{4}$$

Term $\dfrac{\partial^2 y}{\partial t^2}$ represents vertical acceleration of the moving object. Eq. (4) is valid if the moving mass has low speed. If the moving mass has high speed, Eq. (5) considering full acceleration term (i.e. $\frac{d^2 y}{dt^2}=\frac{\partial^2 y}{\partial t^2}+c^2\frac{\partial^2 y}{\partial x^2}+2c\frac{\partial^2 y}{\partial t\partial x}$), must be used.

$$EI\frac{\partial^4 y}{\partial x^4}+2\mu\omega_b\frac{\partial y}{\partial t}+\mu\frac{\partial^2 y}{\partial t^2}=-M\left[\underbrace{c^2\frac{\partial^2 y}{\partial x^2}+2c\frac{\partial^2 y}{\partial t\partial x}+\frac{\partial^2 y}{\partial t^2}}_{\frac{d^2 y}{dt^2}}+g\right]\delta(x-X) \tag{5}$$

Where c is the vehicle speed (Fryba 1972).

If there are some springs and dampers between the moving object and the beam surface, the problem becomes more complicated. The equations of motion for this kind of system, which is called a moving oscillator, can be expressed in the form (Cantero *et al.* 2009)

$$EI\frac{\partial^4 y}{\partial x^4}+2\mu\omega_b\frac{\partial y}{\partial t}+\mu\frac{\partial^2 y}{\partial t^2}=\sum_{i=1}^{n}\delta(x_i-ct)\ F_{ti}(t) \tag{6}$$

$$\boldsymbol{M}\ddot{\boldsymbol{u}}+\boldsymbol{C}\dot{\boldsymbol{u}}+\boldsymbol{K}\boldsymbol{u}=\boldsymbol{F} \tag{7}$$

Where $\boldsymbol{M}$ is the mass matrix, $\boldsymbol{C}$ is the damping matrix and $\boldsymbol{K}$ is the stiffness matrix of the suspension system. $\boldsymbol{u}$ is the vector of DOF's displacement of the system. $\boldsymbol{F}$ is the force vector between the moving object and the beam surface and is a function of both $y(x,t)$ and $\boldsymbol{u}$. The dimension of mass, damping and stiffness matrices is the same as the number of DOF of the system. The main difficulty in this problem is that Eqs. (6) and (7) are coupled and must be solved simultaneously.

3. Bridge model considering congestion

Regarding Hamilton's principle, the governing equation of the Euler-Bernoulli beam of length L, second moment of area I, modulus of elasticity E and constant mass per unit length μ, can be written as

$$EI\frac{\partial^4 y(x,t)}{\partial x^4}+\mu\frac{\partial^2 y(x,t)}{\partial t^2}+2\mu\omega_b\frac{\partial y(x,t)}{\partial t}=F(x,t) \tag{8}$$

Where $y(x,t)$ is the vertical displacement of the beam due to the force $F(x,t)$ at section x and time t. ω_b is the damped circular frequency and for small damping ratios ξ, it is given by (Cantero *et al*. 2009)

$$\omega_b = \frac{\xi}{\sqrt{1-\xi^2}}\omega_j \approx \xi\omega_j \tag{9}$$

$$\omega_j^{\ 2} = \frac{j^4\pi^4}{L^4}\frac{EI}{\mu} \tag{10}$$

$$\omega_j = j^2\omega_1 \tag{11}$$

Where ω_j are natural frequencies of the bridge.

For a force moving at speed c the term $F(x,t)$ in Eq. (8) must be replaced by $\delta(x-ct)F(x,t)$, where δ is the Dirac function.

As a result, for a system with two trucks with n and m axles, the governing equation can be written as

$$EI\frac{\partial^4 y(x,t)}{\partial x^4} + \mu\frac{\partial^2 y(x,t)}{\partial t^2} + 2\mu\omega_b\frac{\partial y(x,t)}{\partial t} = \sum_{i=1}^{n}\delta(x_i - c_1 t)F_{ti}(t)\Bigg|_{vehicle\ 1} + \sum_{i=1}^{m}\delta(x_i - c_2 t)F_{ti}(t)\Bigg|_{vehicle\ 2} \tag{12}$$

For a beam carrying two vehicles at different speeds and different locations, the equations of motion of the vehicle models, Eq. (7), can be expressed in the form

$$\boldsymbol{M_1\ddot{u}_1} + \boldsymbol{C_1\dot{u}_1} + \boldsymbol{K_1u_1} = \boldsymbol{F_1} \tag{13}$$

$$\boldsymbol{M_2\ddot{u}_2} + \boldsymbol{C_2\dot{u}_2} + \boldsymbol{K_2u_2} = \boldsymbol{F_2} \tag{14}$$

Where $\boldsymbol{M_1}$ and $\boldsymbol{M_2}$ are mass matrices, $\boldsymbol{C_1}$ and $\boldsymbol{C_2}$ are damping matrices, $\boldsymbol{K_1}$ and $\boldsymbol{K_2}$ are stiffness matrices of the two vehicle models. $\boldsymbol{u_1}$, $\boldsymbol{u_2}$, $\boldsymbol{F_1}$ and $\boldsymbol{F_2}$ are vectors of generalized coordinates and forces for each vehicle model.

The vehicle tires are prevented from uplift (negative force) by the following condition

$$F_{i,1} = K_{tire,i,1}\left(y_{veh.,i,1} - y_{bridge,i,1} + r_{i,1}\right) \geq 0 \quad \& \quad F_{i,2} = K_{tire,i,2}\left(y_{veh.,i,2} - y_{bridge,i,2} + r_{i,2}\right) \geq 0 \tag{15}$$

$$i = 1,2,\ldots,n$$

Where n is the number of vehicle axles and $y_{bridge,i,j}$ is the displacement of the beam and $r_{i,j}$ is the road profile, respectively, underneath the i^{th} axle of j vehicle at instant t. The coupled Eqs. (12), (13), (14) and (15) must be solved simultaneously.

4. Numerical solution

The beam is divided into more than 200 elements depended on different spans. The more the span, the more the element number to reach more accurate results but the analyses last more. Using the finite difference method, Eq. (12) can be solved for an assumed force vector F_{ti} (t) which consists of $\boldsymbol{F_1}$ and $\boldsymbol{F_2}$. In finite difference method, for the estimation of $y^{(4)}(x_n,t)$, i.e., $\frac{\partial^4 y}{\partial x^4}$, the two Eqs. (16) and (17) can be obtained by Taylor expansion. The Eq. (16) estimates $y^{(4)}(x_n,t)$

by the displacement of the five adjacent nodes but the Eq. (17) uses seven adjacent nodes, which is more accurate.

$$y^{(4)}(x_n,t)=\frac{y(x_{n-2},t)-4y(x_{n-1},t)+6y(x_n,t)-4y(x_{n+1},t)+y(x_{n+2},t)}{(\Delta x)^4} \tag{16}$$

$$y^{(4)}(x_n,t)=\frac{-\frac{1}{6}y(x_{n-3},t)+2y(x_{n-2},t)-\frac{13}{2}y(x_{n-1},t)+\frac{28}{3}y(x_n,t)-\frac{13}{2}y(x_{n+1},t)+2y(x_{n+2},t)-\frac{1}{6}y(x_{n+3},t)}{(\Delta x)^4} \tag{17}$$

Where $y^{(4)}(x_n,t)$ is the fourth derivative of vertical displacement with respect to x.

In estimating the second derivative of displacement with respect to time, i.e., $\frac{\partial^2 y(x,t)}{\partial t^2}$, the Eq. (18) can be used.

$$\frac{\partial^2 y(x,t)}{\partial t^2}=\frac{y(x,t_{n-1})-2y(x,t_n)+y(x,t_{n+1})}{\Delta t^2} \tag{18}$$

In addition, $\boldsymbol{F_1}$ and $\boldsymbol{F_2}$ must satisfy the Eqs. (13) and (14). These two equations can be solved by the Wilson-θ method to calculate $\boldsymbol{u_1}$ and $\boldsymbol{u_2}$. The Wilson-θ method is essentially an extension of the linear acceleration method in which a linear variation of acceleration from time t to time t+Δt is assumed (Cantero *et al*. 2009). The equation must be satisfied at time $t_{n+\theta}=t_n+\theta\Delta t$ with $\theta\geq 1$.

$$\boldsymbol{M}\ \ddot{\boldsymbol{u}}_{\boldsymbol{n+\theta}}+\boldsymbol{C}\ \dot{\boldsymbol{u}}_{\boldsymbol{n+\theta}}+\boldsymbol{K}\ \boldsymbol{u}_{\boldsymbol{n+\theta}}=\boldsymbol{F}_{\boldsymbol{n+\theta}} \tag{19}$$

The displacement and velocity at $t_{n+\theta}$ are related to $\boldsymbol{u}_n$, $\dot{\boldsymbol{u}}_n$, $\ddot{\boldsymbol{u}}_n$ by Eqs. (20) and (21).

$$\boldsymbol{u}_{n+\theta}=\boldsymbol{u}_n+\theta\Delta t\dot{\boldsymbol{u}}_n+(\theta\Delta t)^2[0.5-\beta]\ddot{\boldsymbol{u}}_n+(\theta\Delta t)^2\beta\ddot{\boldsymbol{u}}_{n+\theta} \tag{20}$$

$$\dot{\boldsymbol{u}}_{n+\theta}=\dot{\boldsymbol{u}}_n+\theta\Delta t(1-\gamma)\ddot{\boldsymbol{u}}_n+\theta\Delta t\gamma\ddot{\boldsymbol{u}}_{n+\theta} \tag{21}$$

By substituting Eqs. (20) and (21) into Eq. (19), $\ddot{\boldsymbol{u}}_{n+\theta}$ can be found by solving the non-linear equation. The acceleration at t_{n+1} is then deduced from $\ddot{\boldsymbol{u}}_n$ and $\ddot{\boldsymbol{u}}_{n+\theta}$ by linear interpolation.

$$\ddot{\boldsymbol{u}}_{n+1}=\left(1-\frac{1}{\theta}\right)\ddot{\boldsymbol{u}}_n+\left(\frac{1}{\theta}\right)\ddot{\boldsymbol{u}}_{n+\theta} \tag{22}$$

From which the displacement and velocity at t_{n+1} can be obtained by using the standard Newmark formulae.

$$\boldsymbol{u}_{n+1}=\boldsymbol{u}_n+\Delta t\dot{\boldsymbol{u}}_n+\Delta t^2(0.5-\beta)\ddot{\boldsymbol{u}}_n+\Delta t^2\beta\ddot{\boldsymbol{u}}_{n+1} \tag{23}$$

$$\dot{\boldsymbol{u}}_{n+1}=\dot{\boldsymbol{u}}_n+\Delta t(1-\gamma)\ddot{\boldsymbol{u}}_n+\Delta t\gamma\ddot{\boldsymbol{u}}_{n+1} \tag{24}$$

In the Wilson-θ method, it is assumed β=1/6 and γ=1/2 (Cantero *et al*. 2009). The parameter θ is often chosen to be 1.42.

Finally, by using Eq. (15) and displacement vectors, force vector $F_{ti}(t)$ can be found, which would probably not be the same as the $F_{ti}(t)$ assumed at the beginning of the analysis. That $F_{ti}(t)$, obtained by trial and error, is merely a "good" estimate of the accurate value. This process could be done first for each time increments and afterwards for each velocity of truck increments to calculate the DAF and COP in a wide range of velocities. The DAF (Dynamic Amplification Factor) is the ratio of maximum dynamic stress, due to a moving vehicle, to maximum static stress, due to constant weight of the vehicle, near the mid-span of the beam. COP (Critical Observation Point) is defined as the point on the beam where the maximum bending stress occurs.

Different end condition of the beams can be modeled by using different boundary conditions. For the hinged end condition, which is assumed in this paper, the boundary condition is $y = \frac{\partial^2 y}{\partial x^2} = 0$. The algorithm of problem solving process is shown in Fig. 3.

5. Maximum dynamic bending stresses

Regarding strength of materials science, for a beam with symmetric section under bending moment, the equation of the maximum bending stress in a particular beam section is

$$\sigma_{\max}\big|_{Section} = -\frac{M(h/2)}{I} \tag{25}$$

Where I is the second moment of area, M is the bending moment at the specified section and h is the height of the section. In addition, the bending moment and curvature in the beam have a relation

$$M = EIy'' \tag{26}$$

By combining Eqs. (25) and (26), $\sigma_{\max}$ can be expressed in the form

$$\sigma_{\max}\big|_{Section} = -E(h/2)y'' \tag{27}$$

In finite difference method, for the estimation of y'', i.e., $\frac{\partial^2 y}{\partial x^2}$, the two Eqs. (28) and (29) can be obtained by Taylor expansion. The Eq. (28) estimates y'' by the displacement of three adjacent nodes but the Eq. (29) uses five adjacent nodes, which is more accurate and is used in this paper for the internal nodes.

$$y'' = \frac{\partial^2 y(x_n,t_m)}{\partial x^2} = \frac{y(x_{n-1},t_m) - 2y(x_n,t_m) + y(x_{n+1},t_m)}{\Delta x^2} \tag{28}$$

$$y'' = \frac{\partial^2 y(x_n,t_m)}{\partial x^2} = \frac{-y(x_{n-2},t_m) + 16y(x_{n-1},t_m) - 30y(x_n,t_m) + 16y(x_{n+1},t_m) - y(x_{n+2},t_m)}{12(\Delta x)^2} \tag{29}$$

Therefore, to find the maximum bending stress through the beam length, the maximum curvature, i.e., y'', must be found in each time interval.

$$\sigma_{\max}\big|_{beam} = -E(h/2)\left\{\frac{-y(x_{n-2},t_m) + 16y(x_{n-1},t_m) - 30y(x_n,t_m) + 16y(x_{n+1},t_m) - y(x_{n+2},t_m)}{12(\Delta x)^2}\right\}_{\max} \tag{30}$$

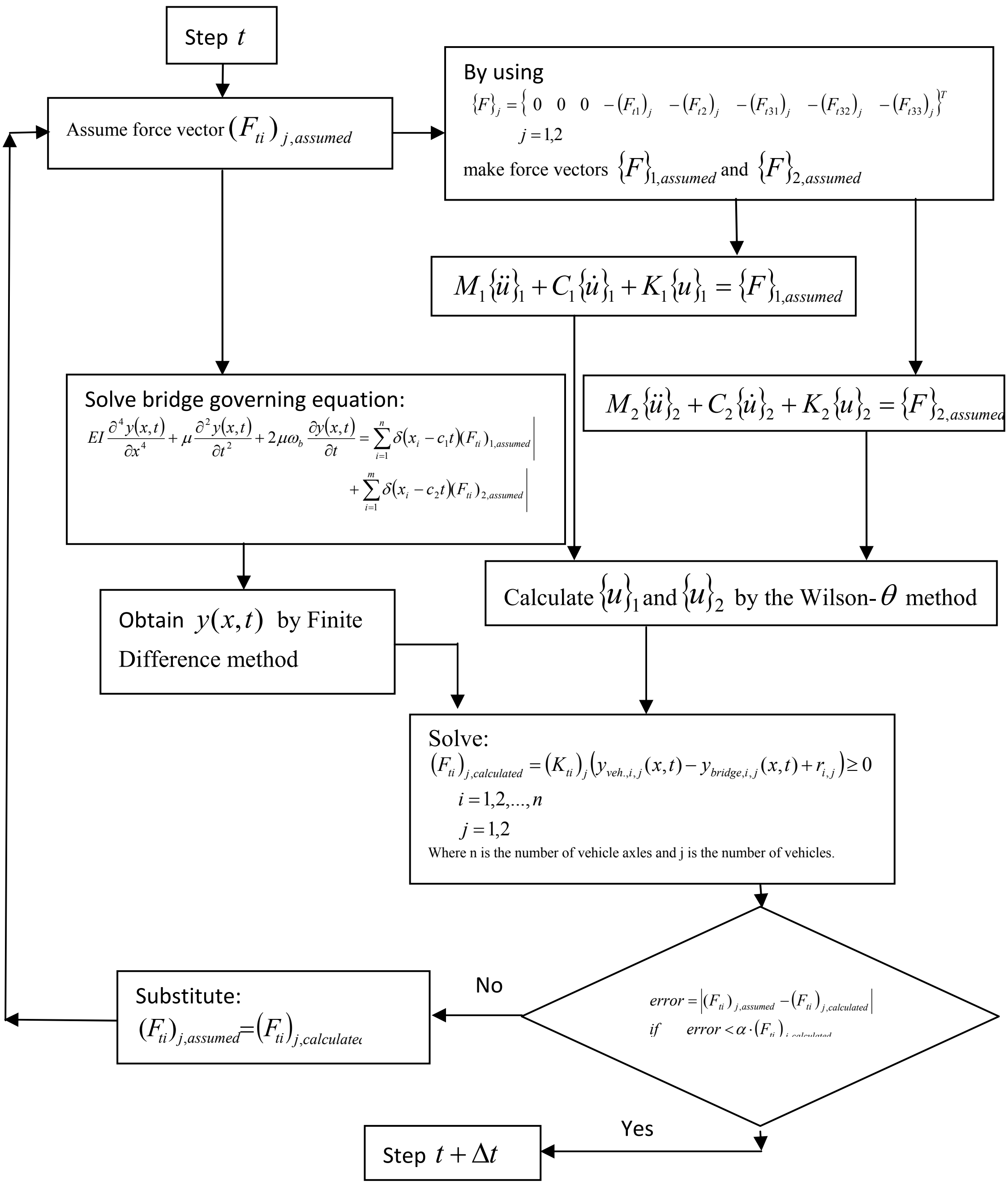

Fig. 3 The algorithm of problem solving process

6. Vehicle model (Case studies)

The aim of the simulation is to consider a beam in two different situations. First, analyzing the bending stresses in the beam as only one vehicle passes over; and second, analyzing again as the

Table 1 Five-axle model parameters

Dimensional data: m	Mass and inertia data
a_1=−0.13	Tractor sprung mass, m_T: 4500 kg
a_2=1.10	Tractor pitch moment of inertia, I_T: 4604 kg.m^2
b_1=0.5	Semi-trailer sprung mass, m_S: 31450 kg
b_2=2.5	Semi-trailer pitch moment of inertia, I_S: 16302 kg.m2
b_{31}=1.30 b_{32}=2.40	Tractor front axle unsprung mass, m_1: 700 kg
b_{33}=3.50	Tractor back axle unsprung mass, m_2: 1100 kg
b_4=4.15 b_5=2.15	Semi-trailer axle unsprung mass, m_{31},m_{32}, m_{33}: 750 kg
Spring rates: kN/m	Viscous damping rates: kNs/m
k_1=400	c_1= 10
k_2=1000	c_2= 10
k_{31}=k_{32}=k_{33}=750	c_{31}=c_{32}=c_{33}=10
k_{t1}=1750	
k_{t2}=3500	
k_{t31}=k_{t32}=k_{t33}=3500	

Table 2 Beam model parameters

Length, L	25	m
Young's modulus, E	3.5×10^{10}	N/m^2
Section inertia, I	1.3901	m^4
Mass per unit length, μ	18358	kg/m
Damping, ξ	3	%

Table 3 Beam model parameters for 15, 35, 70 m span

L = 15 m	Section inertia, I:	0.5273	m^4
	Mass per unit length, m:	28125	kg/m
L = 35 m	Section inertia, I:	3.4162	m^4
	Mass per unit length, m:	21752	kg/m
L =70 m	Section inertia, I:	19.5313	m^4
	Mass per unit length, m:	30752	kg/m

same two vehicles pass over with different speeds and different bridge span lengths.

A five-axle European truck model is used to verify and compare the results with Cantero *et al.* (2009). The vehicle parameters are shown in Table 1.

In Table 2, main beam model parameters, which Cantero *et al.* (2009) used, are listed.

In addition for beam lengths of 15, 35 and 70, DAFs and COPs were also calculated. The section inertia and mass per unit length for each beam length are listed in Table 3. The other parameters, like modulus of elasticity and damping, remain the same as 25 m bridge model.

The analysis for each beam is conducted with two different road profiles. First a smooth profile and second a sinusoidal road profile with 1 cm amplitude and 5 m wave length. The sinusoidal

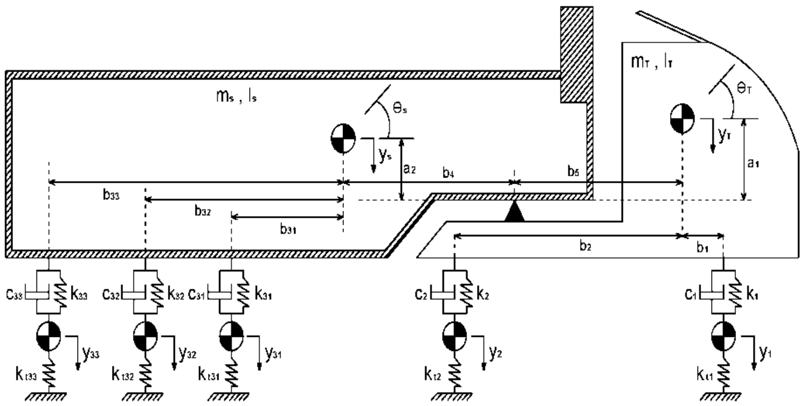

Fig. 4 European truck model

road profiles are calculated because bridge surfaces in real engineering have imperfections and are not smooth because of the construction process.

The vehicle model consists of tractor, semi-trailer and suspensions (Fig. 4). It can be noted that y_S, i.e., the vertical displacement of the semi-trailer, has a geometrical relationship

$$y_S = y_T + b_5\theta_T + b_4\theta_S \tag{31}$$

Where y_T is the vertical displacement of the tractor, y_i (i=1, 2, 31, 32, 33) are the vertical displacement of suspensions, θ_T and θ_s are the pitch of tractor and semi-trailer, respectively.

Consequently, each vehicle model has eight independent degrees of freedom. The equations of motion of the vehicle models can be expressed in the form of Eqs. (13) and (14). $\boldsymbol{u}_1$, $\boldsymbol{u}_2$, $\boldsymbol{F}_1$ and $\boldsymbol{F}_2$ are vectors of generalized coordinates and forces for each vehicle model.

$$\begin{gathered}\boldsymbol{u}_j = \{y_T \quad \theta_T \quad \theta_S \quad y_1 \quad y_2 \quad y_{31} \quad y_{32} \quad y_{33}\}_j^T \\ j = 1,2\end{gathered} \tag{32}$$

$$\begin{gathered}\boldsymbol{F}_j = \{\, 0 \quad 0 \quad 0 \quad -(F_{t1})_j \quad -(F_{t2})_j \quad -(F_{t31})_j \quad -(F_{t32})_j \quad -(F_{t33})_j \,\}^T \\ j = 1,2\end{gathered} \tag{33}$$

Where $(F_{ti})_j$ is the force under the ti^{th} tire of j^{th} vehicle applied to the bridge surface. The tires are prevented from uplift (negative force) by the following condition

$$\begin{gathered}(F_{ti})_j = (K_{ti})_j\left[y_i(t) - y_{br}(x_i, t) + r_i(t)\right]_j \geq 0 \\ i = 1,2,31,32,33 \\ j = 1,2\end{gathered} \tag{34}$$

Where $y_{br}(x_i,t)$ is the displacement of the beam and $r_i(t)_j$ is the road profile, respectively, underneath the i^{th} axle of j vehicle at instant t.

Truck mass matric, $\boldsymbol{M}$, stiffness matric, $\boldsymbol{K}$, and damping matric, $\boldsymbol{C}$, are computed as below (Cantero *et al.* 2009)

$$\boldsymbol{M}=\begin{bmatrix} (m_T+m_S) & b_5m_S & b_4m_S & 0 & 0 & 0 & 0 & 0 \\ b_5m_S & \left(I_T+b_5^2m_S-\dfrac{m_4m_5}{m_4+m_5}a_1^2\right) & \left(b_4b_5m_S-\dfrac{m_4m_5}{m_4+m_5}a_1a_2\right) & 0 & 0 & 0 & 0 & 0 \\ b_4m_S & \left(b_4b_5m_S-\dfrac{m_4m_5}{m_4+m_5}a_1a_2\right) & \left(I_S+b_4^2m_S-\dfrac{m_4m_5}{m_4+m_5}a_2^2\right) & 0 & 0 & 0 & 0 & 0 \\ 0 & 0 & 0 & m_1 & 0 & 0 & 0 & 0 \\ 0 & 0 & 0 & 0 & m_2 & 0 & 0 & 0 \\ 0 & 0 & 0 & 0 & 0 & m_{31} & 0 & 0 \\ 0 & 0 & 0 & 0 & 0 & 0 & m_{32} & 0 \\ 0 & 0 & 0 & 0 & 0 & 0 & 0 & m_{33} \end{bmatrix} \tag{35}$$

$$\boldsymbol{K}=\begin{bmatrix} (k_1+k_2+k_{31}+k_{32}+k_{33}) & [-b_1k_1+b_2k_2+b_5(k_{31}+k_{32}+k_{33})] & [(b_{31}+b_4)k_{31}+(b_{32}+b_4)k_{32}+(b_{33}+b_4)k_{33}] & -k_1 & -k_2 & -k_{31} & -k_{32} & -k_{33} \\ [-b_1k_1+b_2k_2+b_5(k_{31}+k_{32}+k_{33})] & [b_1^2k_1+b_2^2k_2+b_5^2(k_{31}+k_{32}+k_{33})] & b_5[(b_{31}+b_4)k_{31}+(b_{32}+b_4)k_{32}+(b_{33}+b_4)k_{33}] & b_1k_1 & -b_2k_2 & -b_5k_{31} & -b_5k_{32} & -b_5k_{33} \\ [(b_{31}+b_4)k_{31}+(b_{32}+b_4)k_{32}+(b_{33}+b_4)k_{33}] & b_5[(b_{31}+b_4)k_{31}+(b_{32}+b_4)k_{32}+(b_{33}+b_4)k_{33}] & [(b_{31}+b_4)^2k_{31}+(b_{32}+b_4)^2k_{32}+(b_{33}+b_4)^2k_{33}] & 0 & 0 & -(b_{31}+b_4)k_{31} & -(b_{32}+b_4)k_{32} & -(b_{33}+b_4)k_{33} \\ -k_1 & b_1k_1 & 0 & k_1 & 0 & 0 & 0 & 0 \\ -k_2 & -b_2k_2 & 0 & 0 & k_2 & 0 & 0 & 0 \\ -k_{31} & -b_5k_{31} & -(b_{31}+b_4)k_{31} & 0 & 0 & k_{31} & 0 & 0 \\ -k_{32} & -b_5k_{32} & -(b_{32}+b_4)k_{32} & 0 & 0 & 0 & k_{32} & 0 \\ -k_{33} & -b_5k_{33} & -(b_{33}+b_4)k_{33} & 0 & 0 & 0 & 0 & k_{33} \end{bmatrix} \tag{36}$$

$$\boldsymbol{C}=\begin{bmatrix} (c_1+c_2+c_{31}+c_{32}+c_{33}) & [-b_1c_1+b_2c_2+b_5(c_{31}+c_{32}+c_{33})] & [(b_{31}+b_4)c_{31}+(b_{32}+b_4)c_{32}+(b_{33}+b_4)c_{33}] & -c_1 & -c_2 & -c_{31} & -c_{32} & -c_{33} \\ [-b_1c_1+b_2c_2+b_5(c_{31}+c_{32}+c_{33})] & [b_1^2c_1+b_2^2c_2+b_5^2(c_{31}+c_{32}+c_{33})] & b_5[(b_{31}+b_4)c_{31}+(b_{32}+b_4)c_{32}+(b_{33}+b_4)c_{33}] & b_1c_1 & -b_2c_2 & -b_5c_{31} & -b_5c_{32} & -b_5c_{33} \\ [(b_{31}+b_4)c_{31}+(b_{32}+b_4)c_{32}+(b_{33}+b_4)c_{33}] & b_5[(b_{31}+b_4)c_{31}+(b_{32}+b_4)c_{32}+(b_{33}+b_4)c_{33}] & [(b_{31}+b_4)^2c_{31}+(b_{32}+b_4)^2c_{32}+(b_{33}+b_4)^2c_{33}] & 0 & 0 & -(b_{31}+b_4)c_{31} & -(b_{32}+b_4)c_{32} & -(b_{33}+b_4)c_{33} \\ -c_1 & b_1c_1 & 0 & c_1 & 0 & 0 & 0 & 0 \\ -c_2 & -b_2c_2 & 0 & 0 & c_2 & 0 & 0 & 0 \\ -c_{31} & -b_5c_{31} & -(b_{31}+b_4)c_{31} & 0 & 0 & c_{31} & 0 & 0 \\ -c_{32} & -b_5c_{32} & -(b_{32}+b_4)c_{32} & 0 & 0 & 0 & c_{32} & 0 \\ -c_{33} & -b_5c_{33} & -(b_{33}+b_4)c_{33} & 0 & 0 & 0 & 0 & c_{33} \end{bmatrix} \tag{37}$$

7. Model validation

7.1 Comparison with published moving oscillator model

The results obtained by present numerical method have been first compared with analytically simulated results and published results from the literature. Cantero *et al*. (2009) calculated the

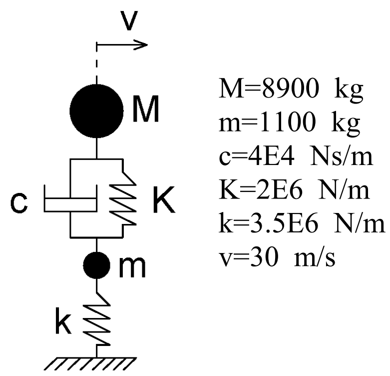

Fig. 5 Moving oscillator model

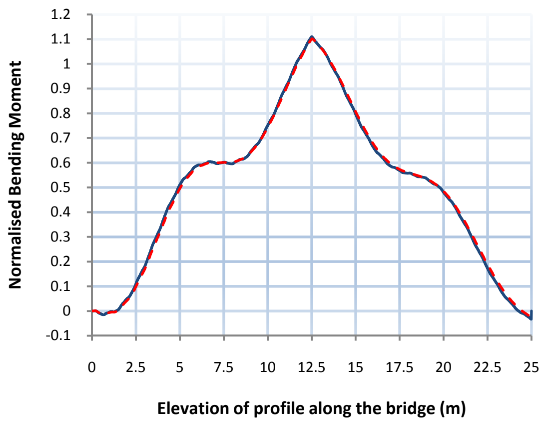

(a) Smooth profile, Cantero *et al*. model (solid) and present model (dashed)

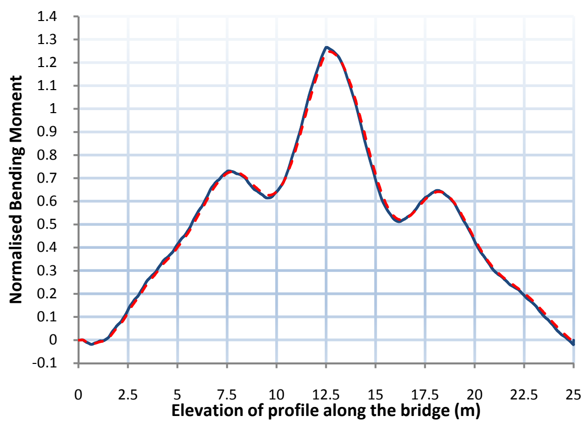

(b) Sinusoidal profile, Cantero *et al*. model (solid) and present model (dashed)

Fig. 6 Verifying the model with Cantero *et al*. (2009) for 25-meter bridge

maximum dynamic stress on simply supported bridges traversed by moving vehicles. Congestion and its influences on DAF were not investigated. So, this analysis, with the same truck and beams properties, is done to compare the results with Cantero *et al*. (2009) to make sure about the approach accuracy. Cantero *et al*. (2009) used the method of finite Fourier integral transformation to separate the Eq. (6) by defining the total bending moment in the beam as the sum of two bending moments, which Fryba (1972) suggested, but in this paper the finite difference method have been used to solve the Eq. (12). Furthermore, Cantero and Obrien have released a benchmark file to verify their results with the other models. They have defined Normalized Bending Moment (NBM) as the ratio of the influence line of bending moment or stress in the middle of the beam to the maximum static bending moment or stress for a moving oscillator problem. They used a moving oscillator problem shown in Fig. 5 and calculated NBM for a 25-meter beam, introduced in Table 2, for two different surface profile: smooth profile and a sinusoidal profile with 1 cm amplitude and 5 m wave length.

By using finite difference method and the algorithm described in section 4, NBMs for the same moving oscillator problem are computed. In Fig. 6, the numerically obtained response (NBM)

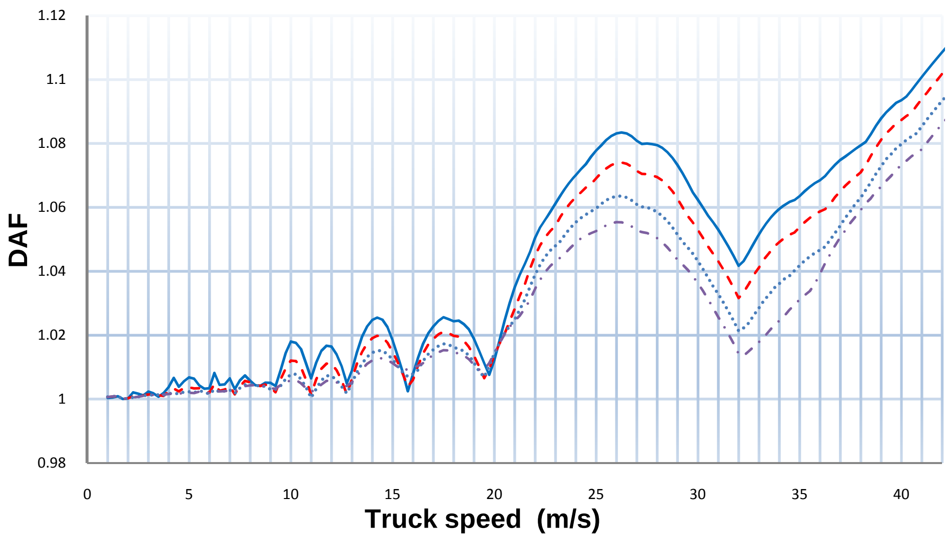

Fig. 7 Damping effect of the bridge (L=25 m) at 1.5% (solid), 3% (dashed), 5% (dotted) and 7% (dash-dotted)

sample has been compared with analytically-numerically simulated response sample found in Cantero *et al*. (2009) for two smooth and sinusoidal road profiles. The comparison of response sample exhibits close agreement between them. The differences are less than 0.5% and are due to different time interval sizes and different approaches. As a result of this accuracy and verification, the described approach is reliable.

7.2 Effect of damping

Finding an appropriate damping value for an actual structure is not easy. To investigate the importance of damping on the bridge response and Dynamic Amplification Factor (DAF), some analyses are performed for a moving truck, described in Fig. 4, on a 25-meter span bridge, describe in Table 2, with different damping ratios (1.5%, 3%, 5% and 7%). The results on DAF are presented in Fig. 7, showing that the lower the damping ratio, the higher the dynamic response but in the same shape, because the bridge is underdamped, i.e., $\xi << 1$.

Cantero *et al*. (2009) calculated the effect of damping on variation of DAF on the same bridge span. Again, the results differ only less than 2% which is negligible. The differences in accuracy between the two are due to different time interval sizes and different approaches.

8. Results and discussions

8.1 Dynamic Amplification Factor (DAF), Critical Observation Point (COP) and Critical Influential Speed (CIS)

Simulations were carried out to analyze the influence of speed, bridge length and road profile

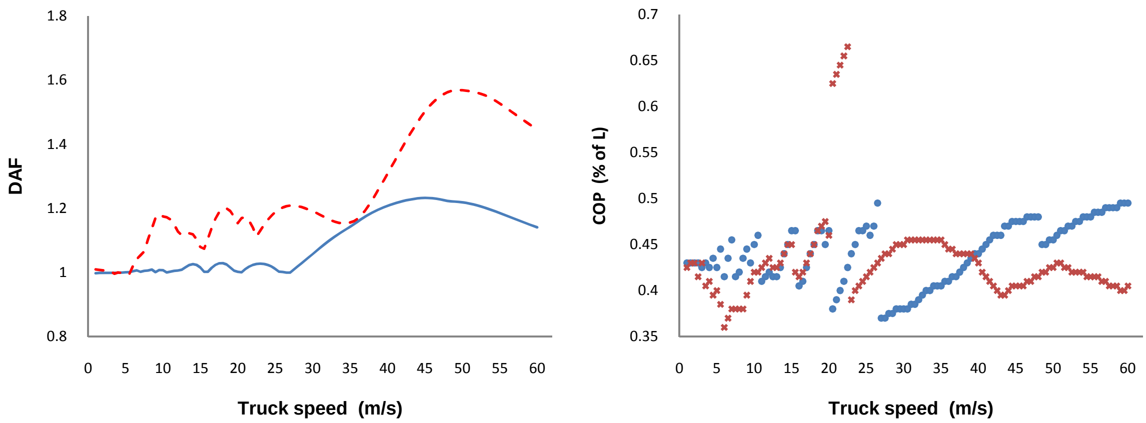

(a) DAF at smooth profile (solid) and sinusoidal (dashed)

(b) COP at smooth profile (dot) and sinusoidal (cross)

Fig. 8 Influence of only one truck speed on DAF and COP of the bridge (*L*=15 m)

on the Dynamic Amplification Factors (DAF's) and Critical Observation Points (COP's). Critical Influential Speed (CIS) is defined as the speed of moving truck in which the beam experiences the maximum dynamic amplification factor (DAF) with respect to time variation. According to the results, CIS can be obtained by scrutinizing the variation of the DAF with respect to variation of the speeds for the moving truck. In order to examine the presented numerical method for moving truck problems and also obtain the CIS values at the same time, the method was carried out for beams, described in Tables 2-3.

The speed is increased in 0.5 m/s intervals between 1 to 60 m/s (3.6 to 216 km/hr) and the damping ratio is assumed 3% in the analyses. The analysis for each beam is conducted with two different road profiles. First a smooth profile and second a sinusoidal road profile with 1 cm amplitude and 5 m wave length. Furthermore, the bridge spans are suggested to be 15, 25, 35 and 70 (4 cases). Each simulation contains a full dynamic problem with 8-DOF moving truck with different speeds on a beam with several nodes and the total passing time divided into more than 2000 intervals. The beam is divided into 200 elements for 15 and 25-meter spans and 300 elements for 35 and 70-meter spans. The time that last the vehicle passes the entire beam is divided into 2000, for short span and high speed, to 7000, for long span and low speed, time intervals depended on the speed of the truck and the beam span. The results are shown in Figs. 8-11

In Fig. 8(a), the influence of speed of one truck passing on a 15-meter length bridge with two different kind of surface profile (smooth and sinusoidal wave) on DAF is presented. As can be seen, the DAF's are nearly 1 in low speed (like static loading) and increases when the speed increases. The DAF is increased at some critical speeds because of the resonance phenomenon, when the loading frequency is near to the natural frequency of the bridge. However, the higher truck speeds, the higher dynamic response of the bridge (DAF) in general. In addition, the sinusoidal wave surface profile rather than smooth profile had considerably effect on having larger DAF. For the 15-meter smooth beam the maximum DAF is 1.233 which occurs at the 45 m/s speed (CIS). In addition, for the same length bridge but with a sinusoidal road surface, the maximum DAF is 1.569 at the CIS=49.5 m/s.

In Fig. 8(b), the influence of the speed of one truck passing on a 15-meter length bridge with

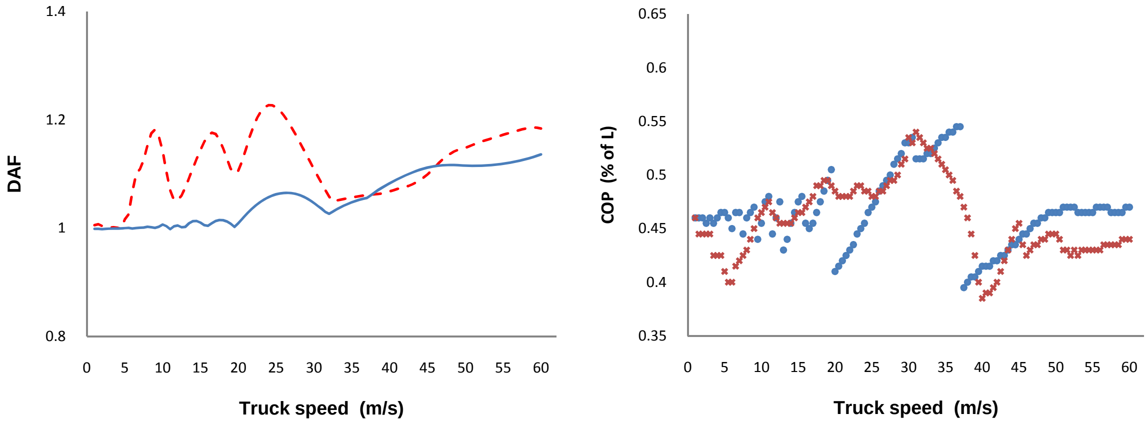

(a) DAF at smooth profile (solid) and sinusoidal (dashed)

(b) COP at smooth profile (dot) and sinusoidal (cross)

Fig. 9 Influence of only one truck speed on DAF and COP of the bridge (L=25 m)

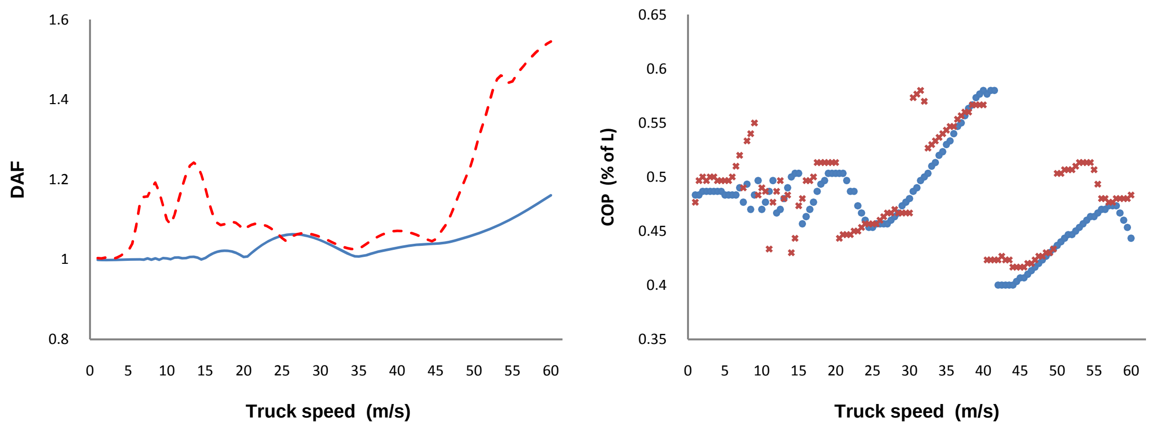

(a) DAF at smooth profile (solid) and sinusoidal (dashed)

(b) COP at smooth profile (dot) and sinusoidal (cross)

Fig. 10 Influence of only one truck speed on DAF and COP of the bridge (L=35 m)

two different kind of surface profile (smooth and sinusoidal wave) on the COP is presented. As can be seen, the location of COPs are not the same for all the truck speeds and are changing in the middle half of the beam span.

The influence of the speed of one truck passing on a 25-meter length bridge on DAF and COP are presented in Fig. 9(a) and 9(b), respectively. Same attitude is seen and in this case for the smooth beam the maximum DAF is 1.136 which occurs at the 60 m/s speed and for the sinusoidal beam, the maximum DAF is 1.227 at the CIS=24 m/s. The results show that the DAF tends to increase in general attitude but some local maximum points occurs which are due to forcing frequencies when they are too close to the natural vibration frequencies of the bridge beam.

Figs. 10-11 present the influence of the speed on a 35-meter length and 70-meter length bridge, respectively. Again, some local maximum points occurs which are due to resonance phenomenon. Furthermore, COPs occur in the middle half of the beam between 0.35-0.65 of bridge span which

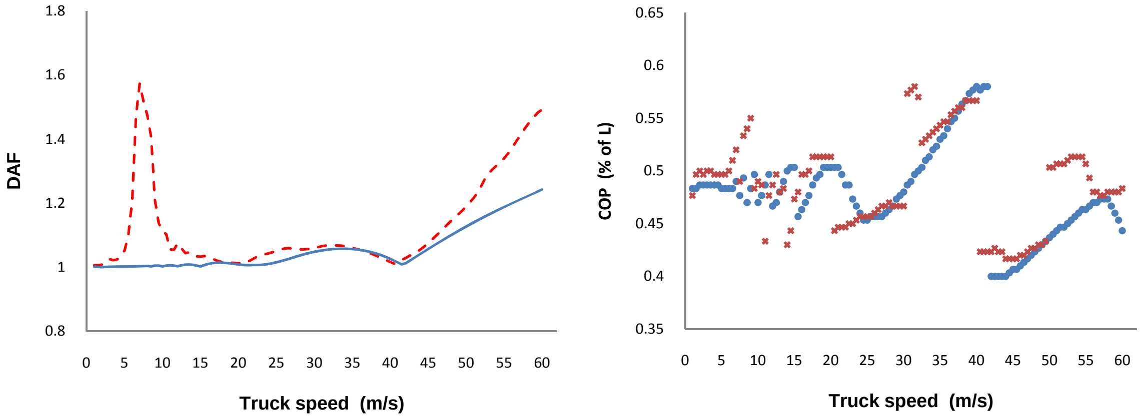

(a) DAF at smooth profile (solid) and sinusoidal (dashed)

(b) COP at smooth profile (dot) and sinusoidal (cross)

Fig. 11 Influence of only one truck speed on DAF and COP of the bridge (L=70 m)

is predictable.

Existing bridge design codes of a conservative nature are still adequate for designing highway bridges at normal traffic speeds. For instance, AASHTO defines a factor called Dynamic Load Allowance (IM). The static effects of the design truck shall be increased by 1.33 for the dynamic load allowance. This approach is conservative at normal truck speeds on a smooth surface profile but when the congestion of trucks with higher speeds moving on an unsmooth road profile is considered the problem becomes more complicated. In this case the dynamic load allowance or impact factor may increase up to more than 1.5 as illustrated in Figs. 8(a), 10(a) and 11(a). Furthermore, based on the results, COP in dynamic analysis is not exactly at the same location as in static analysis.

In addition, it must be noted that the damping effect of soil when in contact with some buried structural components such as footings can decrease the real dynamic load allowance but is not considered in this analysis.

8.2 Effect of bridge span and velocity

The span length of the bridge is an important factor which decides DAF or the impact factor in most of the bridge design codes. Combined effect of bridge span and speed of the truck on DAF is not fully identified. Fig. 12 shows the DAF with variation of velocity and bridge span. It has been found that when the bridge span increases from 15 to 70 m, the maximum DAF decreases by the amount of 10%, when the truck speed is between 30 m/s to 45 m/s. Although increasing span shows a decreasing trend in DAF similar to the earlier studies, when the speed is less than 30 m/s, the increment found in the present case is not very significant for the range of span 15-70 m.

8.3 Effect of bridge surface smoothness and speed

The surface smoothness and speed of the truck are two most influential factors that can cause increased dynamic amplification factor and rapid degradation of the bridge. Bridge dynamic amplification factor has been found by changing bridge surface smoothness for smooth condition to sinusoidal condition as mentioned before with change in truck speed. Fig. 13 shows that sinusoidal condition of road induces more dynamic bending stress in the bridge when the truck moves over it and also can be catalyzed by truck speed. Resonance phenomenon can cause significant increases of DAF in some local critical speeds, for instance near 7 m/s truck speed in 70-meter bridge span.

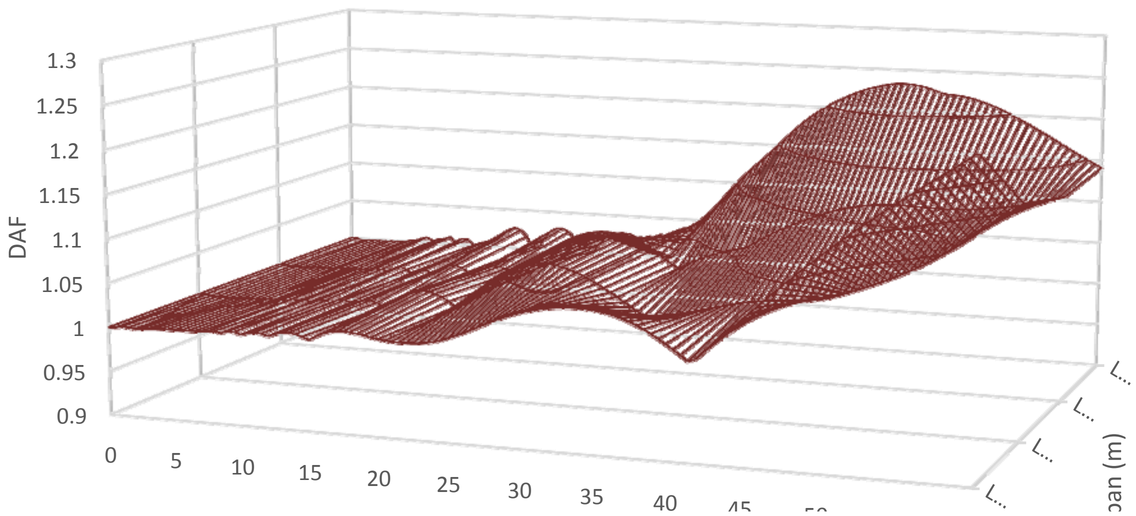

Fig. 12 Dynamic amplification factor with change in truck speed and bridge span

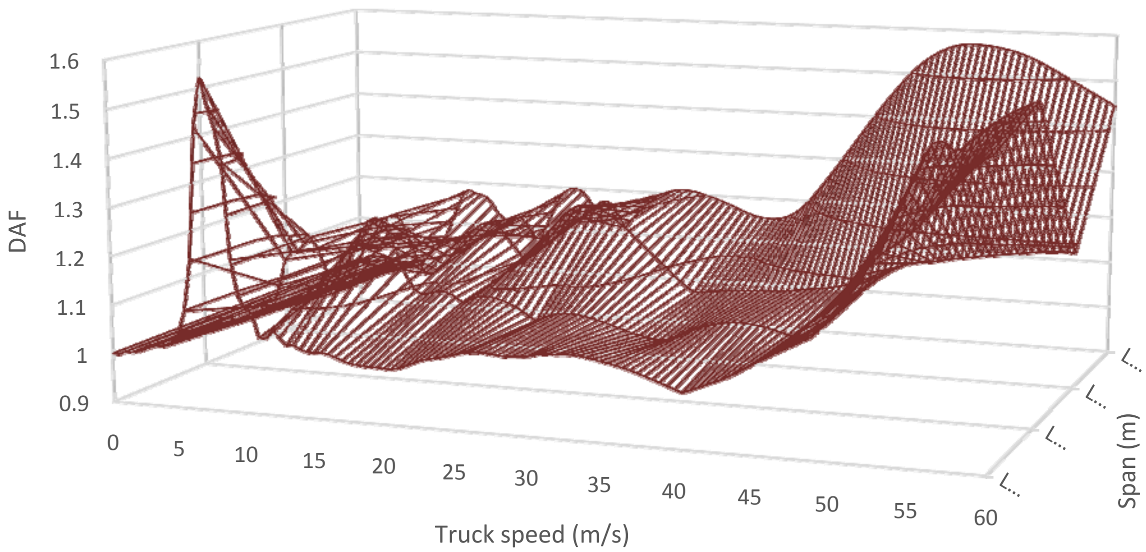

Fig. 13 DAF for a sinusoidal road profile with change in truck speed and bridge span

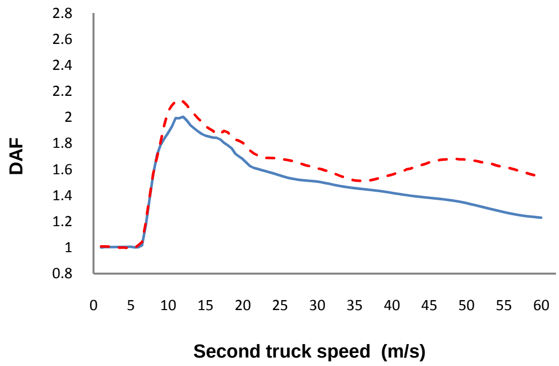

(a) First truck speed=5 m/s (18 km/hr)

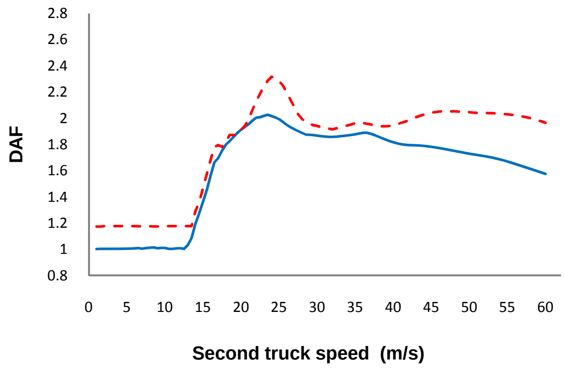

(b) First truck speed=10 m/s (36 km/hr)

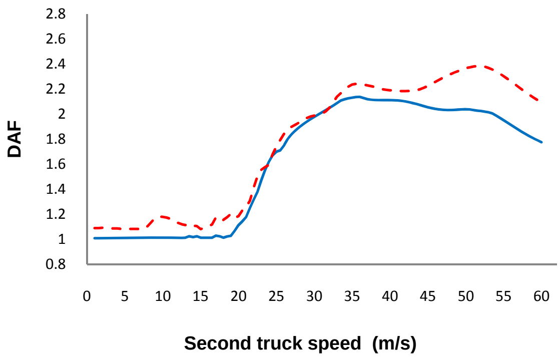

(c) First truck speed=15 m/s (54 km/hr)

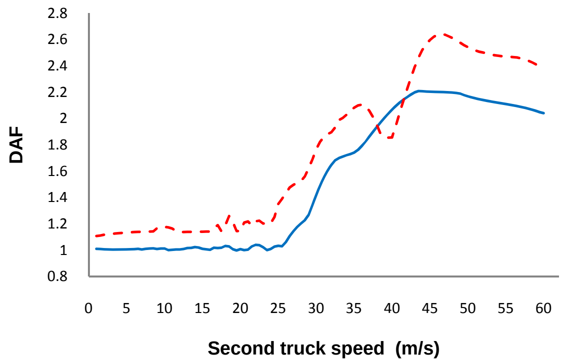

(d) First truck speed=20 m/s (72 km/hr)

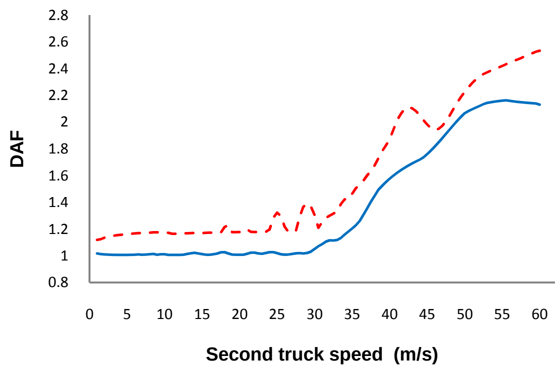

(e) First truck speed=25 m/s (90 km/hr)

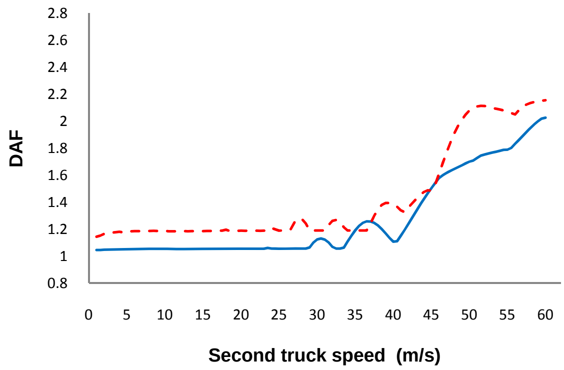

(f) First truck speed=30 m/s (108 km/hr)

Fig. 14 Influence of congestion and second truck speed on DAF of the bridge (L=15 m) at smooth profile (solid) and sinusoidal (dashed)

8.4 Effect of congestion

To consider the congestion, the first truck speeds are 5, 10, 15, 20, 25 and 30 meters per second (6 cases+no congestion case). The second truck speed is increased in 0.5 m/s intervals between 1 to 60 m/s (119 cases). The bridge spans are suggested to be 15, 25, 35 and 70 (4 cases) and two different kinds of surface profile (smooth and sinusoidal wave) are considered. So, the number of moving truck simulations were therefore 7×119×4×2=6664.

Again, each simulation contained a full dynamic problem with 8-DOF moving truck with different speeds on a beam with several nodes and the total passing time divided into more than 2000 intervals. Furthermore, the beam is divided into 200 elements for 15 and 25-meter spans and 300 elements for 35 and 70-meter spans. The time that last the vehicle passes the entire beam is divided into 2000, for short span and high speed, to 7000, for long span and low speed, time intervals depended on the speed of the truck and the beam span. The initial front to front distance between the two trucks is assumed to be 20 meters which varied during the motion because of their different speeds. The results are presented in Figs. 14-17.

Figs. 14(a)-(f), show the influence of congestion and second truck speed on DAF of the bridge for 15-meter length bridge having two different road profile: smooth profile (solid) and sinusoidal profile (dashed). As can be seen, the DAF tends to increase in general attitude but some local maximum points could be seen which were due to forcing frequencies which are too close to the natural vibration frequencies of the bridge beam.

Fig. 15 shows the effect of congestion and second truck speed on DAF of the bridge for 25-meter bridge.

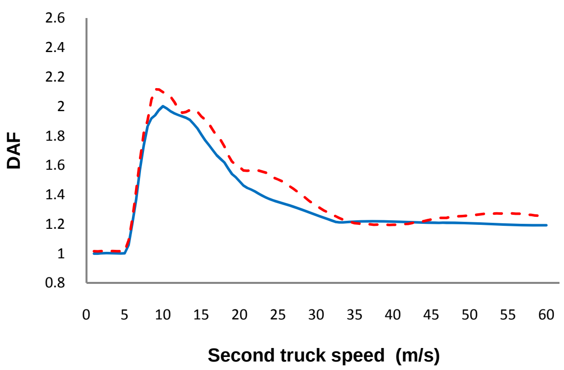

(a) First truck speed=5 m/s (18 km/hr)

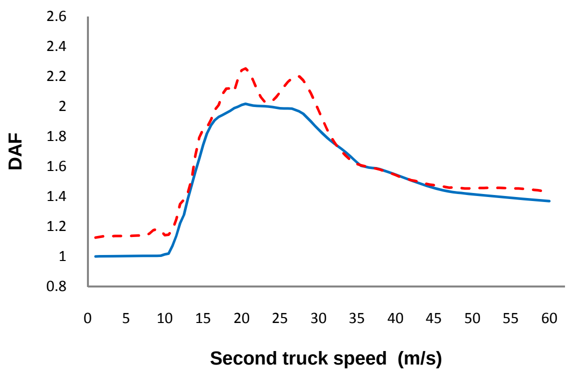

(b) First truck speed=10 m/s (36 km/hr)

(c) First truck speed=15 m/s (54 km/hr)

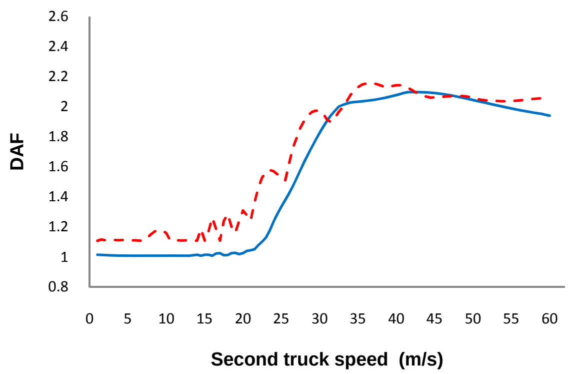

(d) First truck speed= 20 m/s (72 km/hr)

Fig. 15 Influence of congestion and second truck speed on DAF of the bridge (L=25 m) at smooth profile (solid) and sinusoidal (dashed)

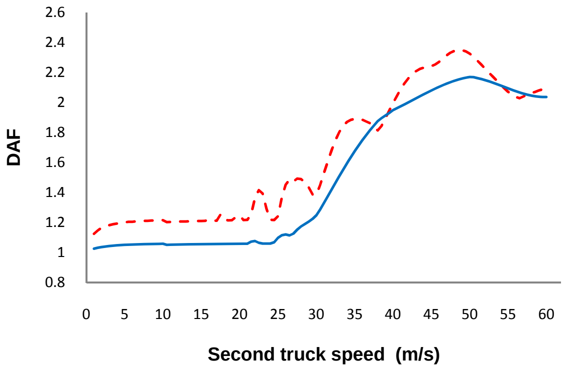

(e) First truck speed=25 m/s (90 km/hr)

(f) First truck speed=30 m/s (108 km/hr)

Fig. 15 Continued

Figs. 16-17 present the influence of congestion and speed on 35-meter length and 70-meter length bridge, respectively. Discussing about the obtained results considering congestion is in the next section (see section 8.5).

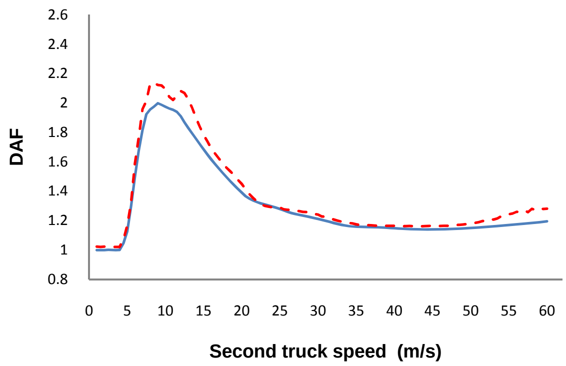

(a) First truck speed=5 m/s (18 km/hr)

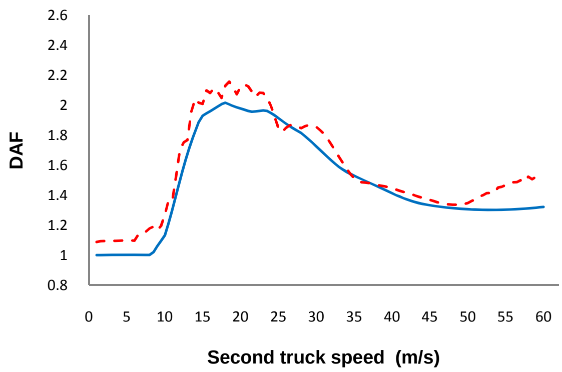

(b) First truck speed=10 m/s (36 km/hr)

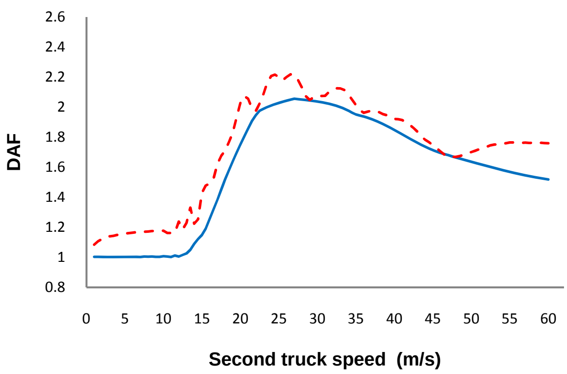

(c) First truck speed=15 m/s (54 km/hr)

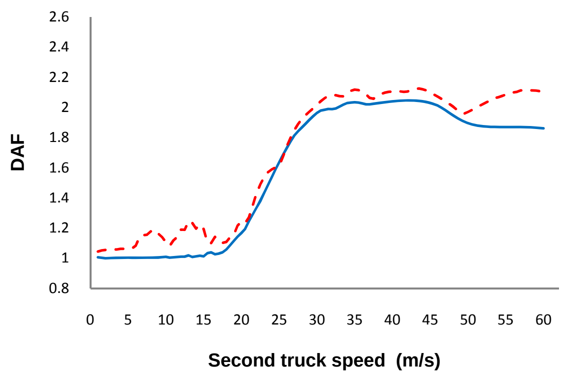

(d) First truck speed=20 m/s (72 km/hr)

Fig. 16 Influence of congestion and second truck speed on DAF of the bridge (L=35 m) at smooth profile (solid) and sinusoidal (dashed)

(e) First truck speed=25 m/s (90 km/hr)

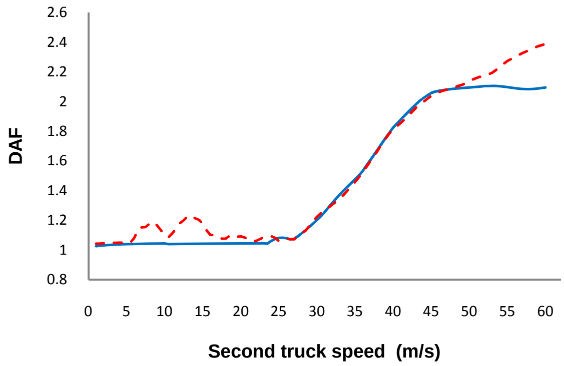

(f) First truck speed=30 m/s (108 km/hr)

Fig. 16 Continued

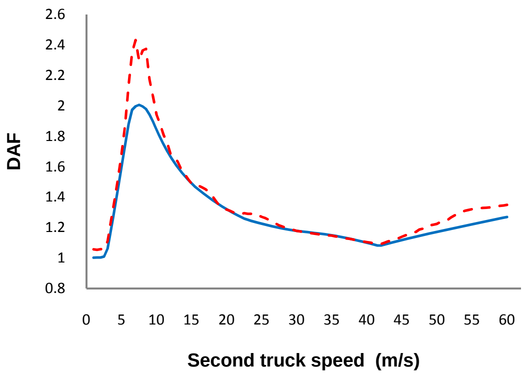

(a) First truck speed=5 m/s (18 km/hr)

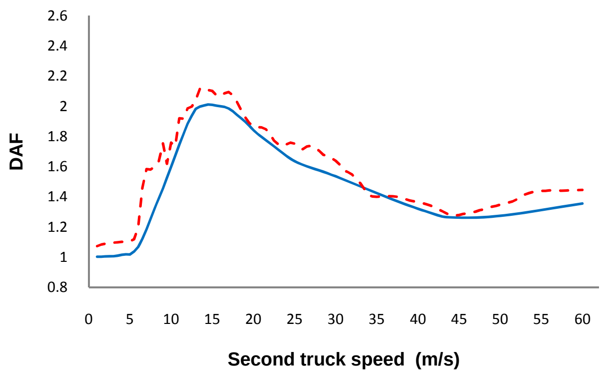

(b) First truck speed=10 m/s (36 km/hr)

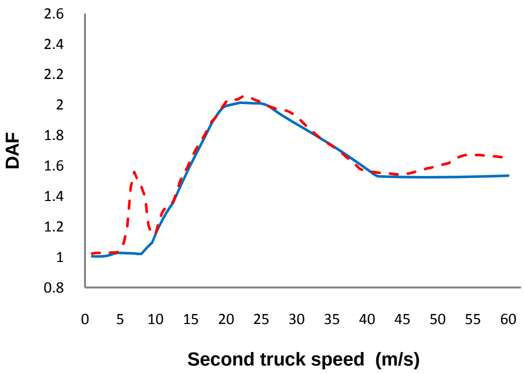

(c) First truck speed=15 m/s (54 km/hr)

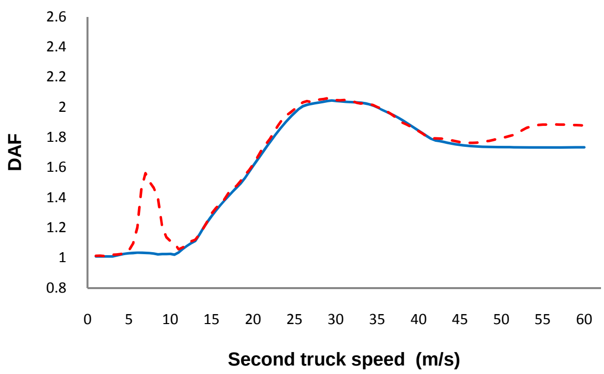

(d) First truck speed=20 m/s (72 km/hr)

Fig. 17 Influence of congestion and second truck speed on DAF of the bridge (L=70 m) at smooth profile (solid) and sinusoidal (dashed)

8.5 DAF variation by congestion, different truck speeds and bridge spans

The results considering congestion are summarized in Table 4 for the two different road

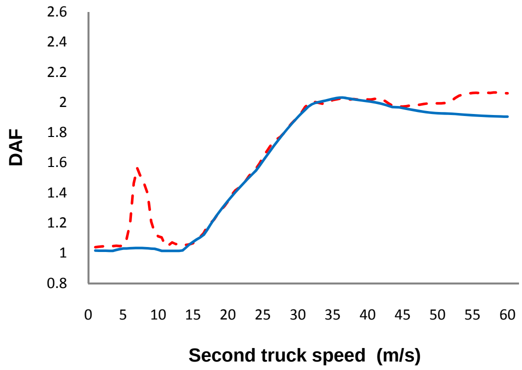

(e) First truck speed=25 m/s (90 km/hr)

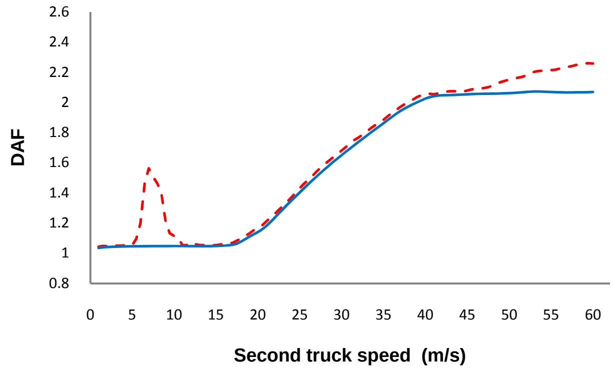

(f) First truck speed=30 m/s (108 km/hr)

Fig. 17 Continued

Table 4 The summary of results and the maximum DAF and CIS of different bridge spans and truck speeds

			L=15 m		*L*=25 m		*L*=35 m		*L*=70 m	
			DAF_{max}	V_1 at DAF_{max} m/s	DAF_{max}	V_1 at DAF_{max} m/s	DAF_{max}	V_1 at DAF_{max} m/s	DAF_{max}	V_1 at DAF_{max} m/s
Second truck speed	v_2=0	Smooth	1.233	45.0	1.136	60.0	1.161	60.0	1.243	60.0
		Sinusoidal	1.569	49.5	1.227	24.0	1.546	60.0	1.573	7.0
	v_2=5 m/s	Smooth	2.005	12.0	2.002	10.0	1.999	9.0	2.006	7.5
		Sinusoidal	2.125	11.0	2.117	9.0	2.138	8.5	2.432	7.0
	v_2=10 m/s	Smooth	2.027	23.5	2.018	20.5	2.016	18.0	2.012	14.5
		Sinusoidal	2.317	24.0	2.254	20.5	2.158	18.5	2.117	13.5
	v_2=15 m/s	Smooth	2.137	36.0	2.055	30.0	2.057	27.0	2.016	22.0
		Sinusoidal	2.383	51.5	2.211	31.0	2.218	26.5	2.060	22.5
	v_2=20 m/s	Smooth	2.208	43.5	2.097	42.5	2.046	42.0	2.045	29.5
		Sinusoidal	2.641	46.5	2.157	36.5	2.126	43.5	2.060	29.0
	v_2=25 m/s	Smooth	2.164	55.5	2.171	50.0	2.112	45.5	2.033	36.0
		Sinusoidal	2.535	60.0	2.350	49.0	2.284	60.0	2.066	59.0
	v_2=30 m/s	Smooth	2.027	60.0	2.157	56.5	2.106	53.5	2.073	53.5
		Sinusoidal	2.155	60.0	2.257	57.5	2.390	60.0	2.260	59.5

profiles. One of the most important parts of the results is the critical influential speed and its relevant DAF.

Since dynamic amplification factor depends on several variables, in this section the results of congestion considering different speeds for the two trucks moving simultaneously on the bridge are investigated. The first row of Table 4 shows the results without considering congestion and only one truck is passing on the bridge. In this case for the smooth road profile, it is seen that existing bridge design codes, with defined DAF as 1.33, are still adequate for designing highway bridges but in the case of sinusoidal road impact factor may be increased up to 1.5, so the

AASHTO is not conservative here, based on performed case studies. It is obvious that these outcomes are not general and need more experimental researches.

The other rows of Table 4 show the DAF for the congestion of two trucks moving simultaneously with two different road profile. It has been found that when the congestion is considered, dynamic amplification factor increases up to the amount of 2 or more, irrespective of bridges span. Although the codes consider a minimum distance between the heavy trucks moving on the bridge, but if the bridge to be designed, is in an area where the congestion of high-speed trucks is probable, the bigger DAF should be chosen by the designer with the help of analytical or numerical methods, for instance the present approach. This methods need more efforts in comparison with using simple values for DAF from the codes, but in some cases it is unavoidable.

To emphasis, it must be mentioned that some of the presented comments in this section would not be true in general and need more tests and numerical or analytical researches to be imported in future bridge codes.

9. Conclusions

In this paper, a model for simply supported Euler-Bernoulli beams under moving trucks considering congestion was presented. In this model, the governing equation of the beam, by using finite difference method, and the equations of motion of two moving trucks, by using Wilson-θ method as well as the trial and error method, were solved simultaneously. Some test problems (different bridges with different spans, 4 cases, different road profiles, 2 cases, different first truck speeds, 119 cases and different second truck speeds, 7 cases, so 6664 cases in total) for different bridges were solved by this algorithm and the results were compared to the results obtained by Cantero *et al*. (2009). Good agreement was observed in the case of moving oscillator problem as well as damping effect on DAFs which were analyzed by Cantero *et al*. (2009). This approximate technique can be applied to beam structures and bridges which are subjected to moving vehicle loading.

• This paper presents an algorithm to solve the governing equation of the bridge as well as the equations of motions of two real European trucks with different speeds, simultaneously. Furthermore, this paper shows the variation of maximum dynamic stress during the passing of one or two trucks at different speeds. The congestion effect on the maximum dynamic stress of bridges can make a significant difference in magnitude.

• Existing bridge design codes which have a conservative nature but are still adequate for designing highway bridges at normal traffic speeds. For instance, the AASHTO defines a factor called Dynamic Load Allowance (IM). The static effects of the design truck shall be increased by 1.33 for dynamic load allowance. This approach is conservative at normal truck speeds on a smooth surface profile but when the congestion of trucks with higher speeds moving on an unsmooth road profile is considered the problem becomes more complicated. In this case the dynamic load allowance or impact factor may increase up to 2.2 as illustrated in the article.

• Where vehicle speeds are considerably higher, for example in the case of railway bridges which have more than one railway line or in the case of multiple lane highway bridges where congestion is probable, based on case studies investigated in this paper, the current designing codes may predict the dynamic stresses lower than actual stresses and the consequences of a full length analysis must be used to design safe bridges. In other words, if the bridge to be designed, is in an area where the congestion of high-speed trucks is probable, the bigger DAF should be chosen by the designer with the help of analytical or numerical methods, for instance the present approach.

• It has been found that when the bridge span increases from 15 to 70 m, the maximum DAF decreases by the amount of 10%, when the truck speed is between 30 m/s to 45 m/s. Although increasing span shows a decreasing trend in DAF similar to the earlier studies, when the speed is less than 30 m/s, the increment found in the present case is not very significant for the range of span 15-70 m.

• Based on the results, COP in dynamic analysis is not exactly at the same location as in static analysis. Therefore, the structural and design engineers should attend this point in their designs.

• Since dynamic amplification factor depends on several variables, resonance phenomenon can make a significant differences in the magnitude of DAF at some local critical speeds.

• Regarding trucks and trains industry improvements and transportation developments, designing high-speed bridges will be needed in near future. Consequently, the new bridges and highways codes should make changes in their bodies based on new researches correlated with experiments, either in situ or on lab models, particularly in calculating DAF.

Finally, it must be noted that the damping effect of soil when in contact with some buried structural components such as footing can decrease the real dynamic load allowance but is not considered in this article.

References

Akin, J.E. and Mofid, M. (1989), “Numerical solution for response of beams with moving mass”, *ASCE J. Struct. Eng.*, **115**(1), 120-130.

American Association of State Highway and Transportation Officials (2012), *Standard Specification for Highway Bridges, SI Units 6th edition*, Washington DC.

British Standards Institution (2003), *Eurocode 1: Actions on Structures, Part 2: Traffic Loads on Bridges*, BS EN 1991-2, London.

Cantero, D., Gonzalez, A. and Obrien, E.J. (2009), “Maximum dynamic stress on bridges traversed by moving loads”, *Bridge Eng.*, **162**(2), 75-85.

Chang, K., Kim, C. and Kawatani, M. (2014), “Feasibility investigation for a bridge damage identification method through moving vehicle laboratory experiment”, *Struct. Infrast. Eng.*, **10**(3), 328-345.

Dehestani, M., Mofid, M. and Vafai, A. (2009), “Investigation of critical influential speed for moving mass problems on beams”, *Appl. Math. Model.*, **33**(10), 3885-3895.

Fryba, L. (1972), *Vibration of Solids and Structures under Moving Loads*, Noordhoff, Groningen, The Netherlands.

Gasic, V., Zrnic, N., Obradovic, A. and Bosnjak, S. (2011), “Considering of moving oscillator problem in dynamic responses of bridge cranes”, *FME Tran.*, **39**(1), 17-24.

Mofid, M., Tehranchi, A. and Ostadhossein, A. (2010), “On the viscoelastic beam subjected to moving mass”, *Adv. Eng. Softw.*, **41**(2), 240-247.

O’Connor, C. and Shaw, P.A. (2000), *Bridge Loads, An International Perspective*, Spon Press, London.

Siddiqui, S.A., Golnaraghi, M.F. and Heppler, G.R. (1998), “Dynamics of a flexible cantilever beam carrying a moving mass”, *Nonlin. Dyn.*, **15**(2), 137-154.

Siddiqui, S., Golnaraghi, M. and Heppler, G. (2003), “Large free vibrations of a beam carrying a moving mass”, *Int. J. Nonlin. Mech.*, **38**(10), 1481-1493.

Wang, Y.M. (1998), “The dynamical analysis of a finite inextensible beam with an attached accelerating mass”, *Int. J. Solid. Struct.*, **35** (9-10), 831-854.

Wang, Y.M. (2005), “the transient dynamics of multiple accelerating/decelerating masses traveling on an initially curved beam", *J. Sound Vib.*, **286**(1-2), 207-228.

Zhang, Q., Jankowski, L. and Duan, Z. (2013), "Simultaneous identification of moving vehicles and bridge damage considering road rough surface", *Math. Prob. Eng.*, Article ID 963424.

Zheng, D.Y., Au, F.T. and Cheung, Y.K. (2000), "Vibration of vehicle on compressed rail on viscoelastic foundation", *ASCE J. Eng. Mech.*, **126**(11), 1141-1147.

CC